Featured in Physics

Pedestrian stepping dynamics in single-file movement

Yi Ma,[1,*] Ying Ying Sun,[1,†] Eric Wai Ming Lee,[2,‡] and Richard Kowk Kit Yuen[2,§]
[1]*Institute for Disaster Management and Reconstruction, Sichuan University, Chengdu 610065, China*
[2]*Department of Architecture and Civil Engineering, City University of Hong Kong, Kowloon, Hong Kong*

(Received 24 September 2018; published 14 December 2018)

In this paper, we present a pedestrian single-file movement experiment that directly captures the characteristics of the interacting pedestrians' continuous stepping behaviors. We find that the relationship between step length (duration) and spatial headway exhibits piecewise linear behavior: It first increases linearly as the headway increases and then remains constant when the headway exceeds 1.20 m (0.71 m). Three different regimes are observed and defined on the basis of their relationships. The continuous small-step phenomena are found in a strongly constrained regime. We reveal that the relationship between the step duration and the step velocity is nonmonotonous and that the longest duration is seen at a velocity of 1.35 m/s, whereas the relationship between the step length and the step velocity is monotonous and can be well represented by a quartic function. Furthermore, we show that the dependency of the ratio between head displacement and foot displacement in a step on the headway is a piecewise linear relationship. We were interested to find that the ratio is less (greater) than 0.5 when the headway is less (greater) than 1 m. This finding reveals the backward- (forward-) deviating phenomena of the body and can be used to indirectly interpret the differences in some of the results of this paper and previous studies. Finally, we show that step synchronization (asynchronization) is most likely to occur at a headway of 0.76 m (0.51 m). These interesting findings greatly deepen our understanding of basic human stepping behavior.

DOI: 10.1103/PhysRevE.98.062311

I. INTRODUCTION

Pedestrian dynamics is a fascinating research topic for physicists because crowds of pedestrians exhibit various subtle collective effects and self-organized phenomena [1–7], such as arching, clogging, and faster is slower during evacuation; stop-and-go waves in a passage; lane formation in counterflow; stripe formation in crossing flow; and oscillation in counterflow through a bottleneck. Pedestrian dynamics is also an important research topic in engineering because an understanding of the characteristics of pedestrian behavior has great significance in the design of modern pedestrian facilities and the development of management countermeasures for crowds.

The natural walking process of pedestrians is stepwise. An understanding of basic pedestrian stepping behavior is the premise of understanding complex human movement. Single-file crowd movement is widely used to study how pedestrians step [8–19] and can be observed in many natural situations. For example, in a narrow corridor, pedestrians may walk in a line due to the limited lateral space. In a bidirectional pedestrian flow, the flow of pedestrians can give rise to a self-organized lane formation phenomenon that increases traffic efficiency, and single-file movement can be often observed in the segregated lanes. In the single-file movement of pedestrians, the local interactions among pedestrians are mainly longitudinal. It is easier to study how pedestrians step in such settings. Indeed, such experiments have been widely conducted in recent years to decode the characteristics of pedestrian stepping behavior.

Seyfried *et al.* [9] performed an experiment that revealed the linear relationship between the velocity and the inverse of density. Chattaraj *et al.* [10] investigated the cultural differences in this relationship in a similar experiment. Jelić *et al.* [11,12] studied the fundamental diagram and stepping behavior of pedestrians walking in line and revealed the relationships among step variables (e.g., step length, step duration, local velocity, and density) and the synchronization phenomena in stepping dynamics. Chao and co-workers [13,14] investigated the effects of the pedestrians' age on the fundamental diagram and stepping behavior. They analyzed the relationships between velocity and step width, between velocity and step length, and between velocity and stepping time for various age groups and revealed the effects of pedestrian gender and height on stepping law. Wang and co-workers [15,16] investigated the step styles and step characteristics of pedestrians at various densities. Zeng *et al.* [17] revealed the relationship between step length and step frequency under different headways. Fang *et al.* [18] performed experiments that revealed the relationships between step length and density, between step frequency and density, and between step frequency and headway. A single-file experiment concerning stepping behavior was also conducted by Yanagisawa *et al.* [19] to verify their model. Various types of experiments have also been conducted to study pedestrian stepping behavior. Seitz and Köster [20] extracted step length data for

*yima23_c@scu.edu.cn
†Corresponding author: sunying@scu.edu.cn
‡ericlee@cityu.edu.hk
§acehead@cityu.edu.hk

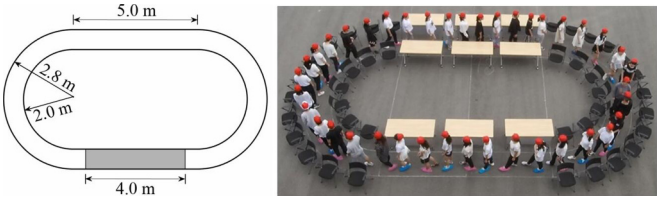

FIG. 1. Schematic of the scenario and a snapshot from the experiment.

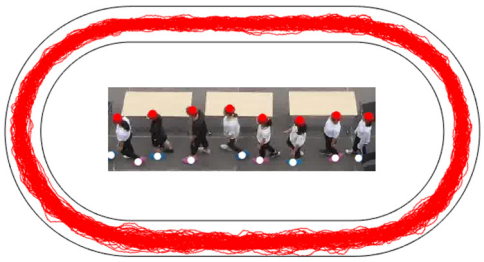

FIG. 2. Trajectories of head motion during the run with 40 participants. The inset is the schematic of the identification of head positions (i.e., the centers of the red points) and foot positions (i.e., the centers of the white points).

pedestrians whereas walking, jogging, and running, and gave a functional relationship between the step length and velocity. Seitz *et al.* [21] studied pedestrian stepping behavior in a two-dimensional environment and found that a change in the walking direction is constrained by the walking speed. Stepping behavior has also been investigated from the perspectives of medicine and sports science [22–24].

From the review of previous studies concerning pedestrian stepping behavior, we noted that their steps were usually tracked by the oscillation of the pedestrians' heads [12,14–17]. The bipedal alternating locomotion of pedestrians has not been directly tracked. As a result, some critical characteristics of stepping behavior may have been missed, and, in particular, the stepping dynamics under foot are not fully clear. The key problem of how pedestrians adapt their footsteps in various situations has not been addressed thoroughly. Seitz and Köster [20] directly measured pedestrians' footsteps, but their measurements were restricted to isolated pedestrians.

Based on these considerations, in this paper, we conduct a well-controlled single-file experiment under laboratory conditions to investigate the characteristics of pedestrian stepping behavior. In particular, we attempt to address how pedestrians step under different headways. This is a single-file experimental study of pedestrian stepping dynamics that captures directly and precisely the characteristics of the continuous stepping behavior of interacting pedestrians. The innovative findings will greatly deepen our understanding of the basic stepping behavior of human beings.

II. EXPERIMENT

The goal of our experiment was to investigate the characteristics of stepping behavior with a particular focus on pedestrians' footsteps in an attempt to reveal the step characteristics in various headway conditions.

The experiment was performed in March 2018 at Sichuan University in Chengdu, China. The experimental scenario (Fig. 1) is a ring corridor consisting of two straight parts (length, 5 m) and two semicircles (outer radius, 2.8 m; inner radius, 2 m). The width of the corridor is 0.8 m, and the length of the measured section shown in the center of the straight parts is 4 m. Note that the lower edge of the measured section is enclosed by a clear white boundary line on the floor. This setting enabled clear observation of the pedestrians' foot motions.

The experiment involved 70 pedestrians; all were students recruited from various schools at Sichuan University. Seven runs were performed with 10, 20, 30, 40, 50, 60, and 70 participants in the corridor. The global density [11,13] varied from 0.40 to 2.82 m^{-1}.

Each participant was equipped with two markers (a hat and a shoe cover with specific colors). The participants were asked to wear a red hat on their head and either a blue or a pink shoe cover on the left foot in alternating fashion. The use of two colors for the shoe covers was to distinguish more clearly the respective feet of two successive pedestrians. Such a marker setting enabled us to track directly and precisely both the head motion and the foot motion of the pedestrians in the experiment.

Note that a shoe cover was used to track only the left feet of the pedestrians because their right feet could not be clearly observed due to occlusion by the body especially in high-density conditions. Fortunately, because the measured section was straight, the stepping law of the left foot under the same headway was generally symmetrical with the stepping law of the right foot.

At the start of each run, the participants were distributed uniformly in the corridor. During each run, the participants were asked to walk in a natural way, not to overtake each other, and not to cross the white boundary line on the outer ring. To collect sufficient data, each run lasted around 3 min.

The whole experiment was recorded with a camcorder at a top-down viewing angle. The resolution of the camcorder was set to 1920×1080, and a frame rate of 25 frames per second was used. Note that the camcorder's viewing angle was not 100% perpendicular but slightly slanted to the ground to enable us to clearly observe both the hats on the heads and the shoe covers on the feet in the video recordings.

The mean-shift clustering algorithm [25,26] was adopted to automatically extract the positions of the hats and shoe covers in each frame. The head positions in real physical space were obtained by transforming the extracted positions of the hats in the video space with the linear transformation method [25,26]. In this manner, the head motion can be tracked directly as shown in Fig. 2. The base plane was then changed to the ground. The foot positions in real physical space were obtained by transforming the extracted positions of the shoe covers in the video space with the linear transformation method. In this manner, the foot motion can be tracked directly.

Note that the position of a pedestrian's foot after linear transformation is precise only when his or her foot is on the ground because the ground is the selected reference plane

during the linear transformation process. However, in the middle of the motion process of a footstep, the foot is not on the ground but lifted up (unless he or she slides the foot along the ground). This suggests that the calculated coordinate of the foot may contain a small amount of error when the foot is in motion. Fortunately, the foot is on the ground at the beginning and end of a footstep, so these small errors do not influence the detection of a footstep's duration.

III. STEP MEASUREMENT

In Refs. [12,14–16], steps were tracked indirectly via oscillation of the head. However, it is possible that the head oscillation did not rigorously coincide with the feet cycles [12]. Thus, we used a direct method to track footsteps.

To track footsteps, the foot's longitudinal motion was approximated by projecting the foot's two-dimensional coordinate to the horizontal central line of the measured section. Figure 3 shows the time-space diagrams of foot motion for the various runs. The moving and motionless states of the foot can be easily observed in terms of the time-space diagrams obtained. Theoretically, in the time-space diagrams, each fraction of the horizontal (blue) line represents that the foot is motionless, whereas each fraction of the oblique (red) line represents that the foot is in motion.

To extract the steps, the longitudinal instantaneous velocity of the foot at the τth frame is calculated

$$v_i(\tau) = \frac{x_i(\tau + \Delta\tau) - x_i(\tau - \Delta\tau)}{2\ \Delta\tau/25}, \tag{1}$$

where $x_i(\tau)$ is the longitudinal coordinate of the foot of pedestrian i at the τth frame. $\Delta\tau$ is the time interval (three frames is used in this paper). The video clips were shot at 25 frames per second. Figure 4(b) shows an exemplary change in the velocity of the foot against time.

Figure 4(b) clearly shows a total of three complete steps. To divide the moving and stopping phases of the foot, the velocity $v = 0.1\,\mathrm{m/s}$ was taken as the threshold [13]. The frame number (τ^s) of the start of one step can be detected automatically if $v_i(\tau^s - 1) < 0.1$ and $v_i(\tau^s) \geqslant 0.1\,\mathrm{m/s}$. In contrast, the frame number (τ^e) of the end of one step can be detected automatically if $v_i(\tau^e) \geqslant 0.1$ and $v_i(\tau^e + 1) < 0.1\,\mathrm{m/s}$. Once the frame numbers of the start and end of each step were obtained, the step duration and length could be calculated directly and easily as shown in Fig. 4(a).

In this way, the steps were fully extracted in terms of the time-space curves shown in Fig. 3. Finally, to guarantee the accuracy of the data and avoid some mistakes during step detection, the frame numbers of the start and end of each step were checked and corrected manually after they were detected automatically. We collected 108, 459, 532, 517, 408, 324, and 128 step samples from the runs with 10, 20, 30, 40, 50, 60, and 70 participants, respectively. Each step corresponds to a fraction of a red line in the time-space diagrams in Fig. 3.

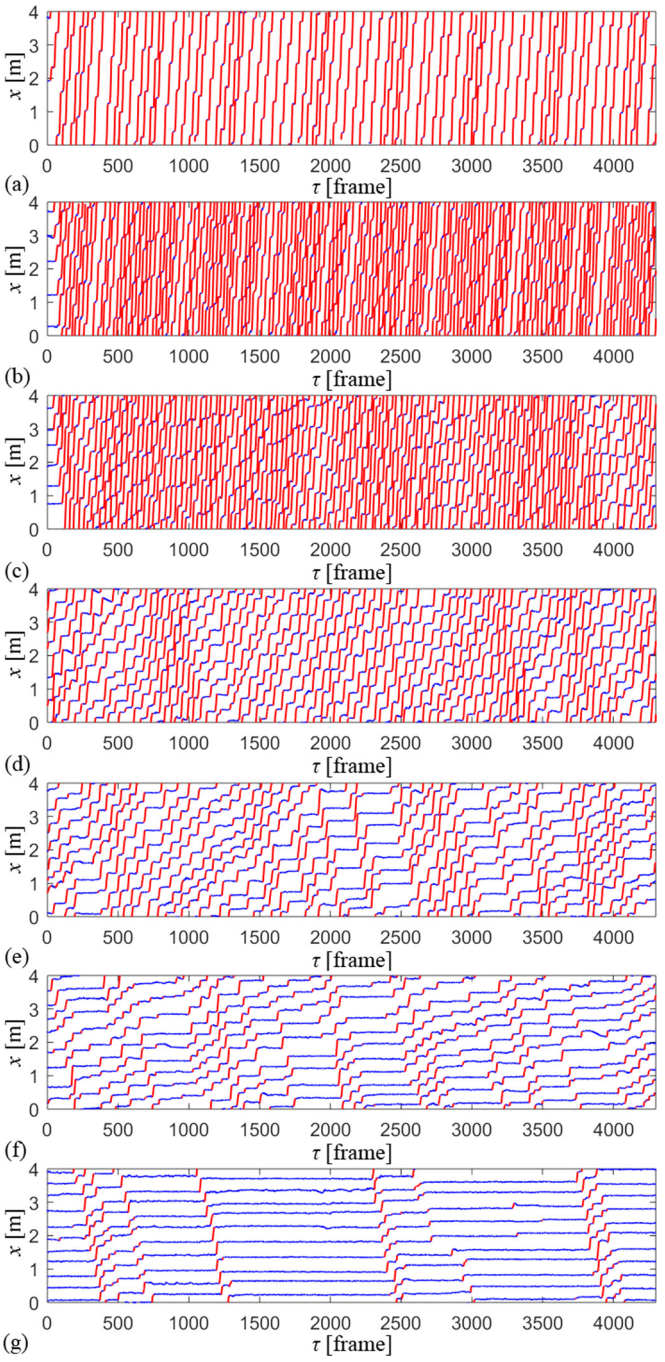

FIG. 3. (a)–(g) Time-space diagrams for runs with 10, 20, 30, 40, 50, 60, and 70 participants, respectively. Each fraction of the horizontal (blue) line represents the foot is standing still, whereas each fraction of the oblique (red) line represents the foot is in motion. Note that, at high densities, such as 70 participants (g), each round of motion after a long stop often comprises a couple of continuous small steps characterized by short step duration and length. We refer to this phenomenon as the small-step phenomenon.

IV. RESULTS

A. Stepping law and small-step phenomenon

In this section, we address the question of how pedestrians adjust their step duration and length under various headways (i.e., the headway-step duration relation and headway-step length relation). Because the frame numbers of the start $(\tau^s_{i,j})$ and end $(\tau^e_{i,k})$ of pedestrian i at the kth step have been obtained, the corresponding step duration $(T_{i,k})$, step length $(l_{i,k})$, and spatial headway $(d_{i,k})$ can be easily

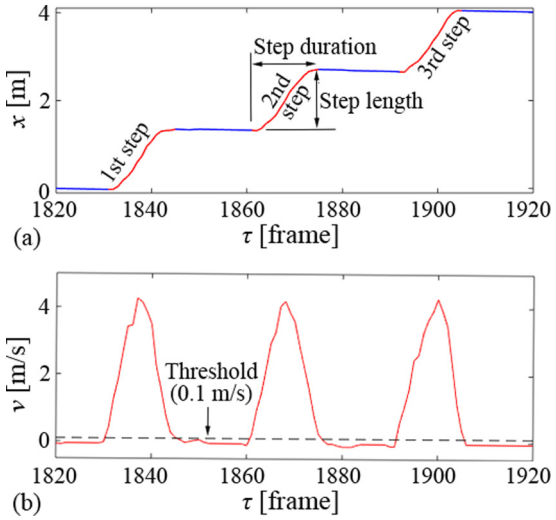

FIG. 4. (a) Time-space diagram of foot motion for a selected pedestrian. Oblique (red) curves represent the obtained steps in terms of the foot's velocity change. (b) Corresponding velocity change in the foot against time.

calculated by

$$T_{i,k} = \frac{\tau^e_{i,k} - \tau^s_{i,k}}{25}, \tag{2}$$

$$l_{i,k} = x_i\left(\tau^e_{i,k}\right) - x_i\left(\tau^s_{i,k}\right), \tag{3}$$

$$d_{i,k} = X_{i-1}\left(\tau^s_{i,k}\right) - X_i\left(\tau^s_{i,k}\right), \tag{4}$$

where the frame rate of the video recordings is 25 per second and $x_i(\tau)$ and $X_i(\tau)$ represent the coordinates of the foot and head, respectively, of pedestrian i at the τth frame.

Figure 5 shows the scatter diagrams for headway and step length and for headway and step duration. To better determine the relationships between headway and step length and between headway and step duration, we used a binning procedure similar to that in Ref. [12] to analyze the data (see Fig. 6). The results are fitted with the following piecewise function:

$$l = \begin{cases} 1.43d - 0.45, & \text{if } d < 1.20\,\text{m}, \\ 1.27, & \text{if } d \geqslant 1.20\,\text{m}, \end{cases} \tag{5}$$

$$T = \begin{cases} 0.82d + 0.04, & \text{if } d < 0.71\,\text{m}, \\ 0.62, & \text{if } d \geqslant 0.71\,\text{m}, \end{cases} \tag{6}$$

where l, T, and d represent the step length, step duration, and headway, respectively.

A comparison of Figs. 6(a) and 6(b) clearly shows that the steady states of the step length and step duration arise at different headways (1.20 and 0.71 m, respectively), which suggests the existence of three different regimes.

(a) Free regime ($d \geqslant 1.20\,\text{m}$). The step duration and step length are both constant (0.62 s and 1.27 m) and thus independent of the headway. This finding suggests that the pedestrian's motion is not constrained by that of the predecessor and that pedestrians can use their preferred stepping pace. Theoretically, pedestrians will not adjust their step duration or step length in this regime.

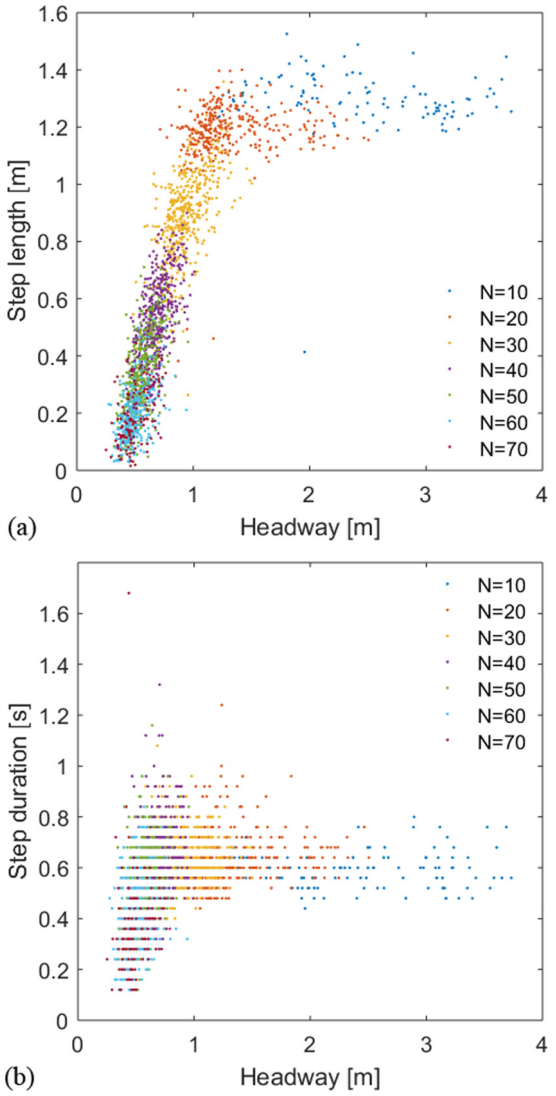

FIG. 5. Scatter diagram of 2476 (a) headway-step length samples and (b) headway-step duration samples.

(b) Weakly constrained regime ($0.71\,\text{m} \leqslant d < 1.20\,\text{m}$). The step length decreases as the headway decreases, whereas the step duration remains constant (0.62 s). This finding

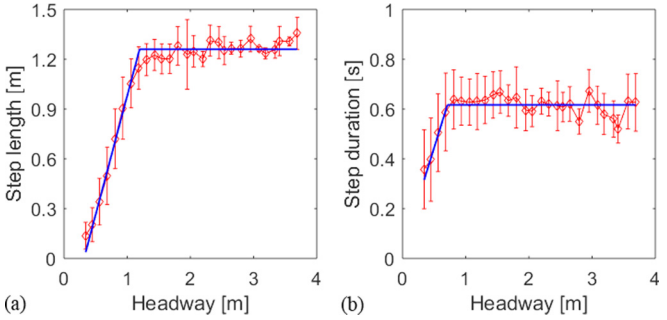

FIG. 6. Binning and fitting results of (a) headway-step length samples and (b) headway-step duration samples.

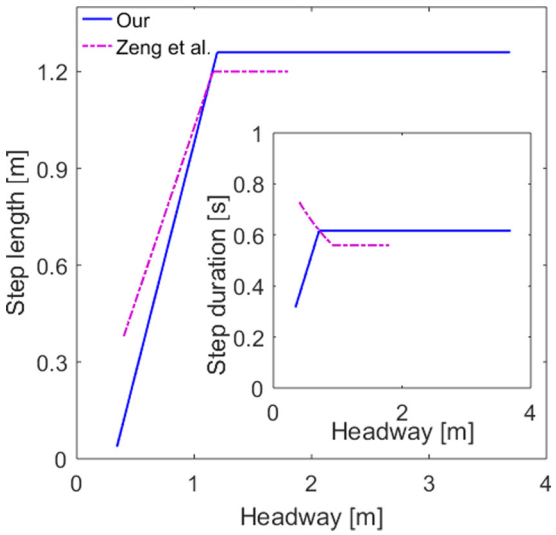

FIG. 7. Comparison of relationships between headway and step length and between headway and step duration (the inset) for our result and those of Zeng *et al.* [17]. Note that the results of Zeng *et al.* [17] have been equivalently converted.

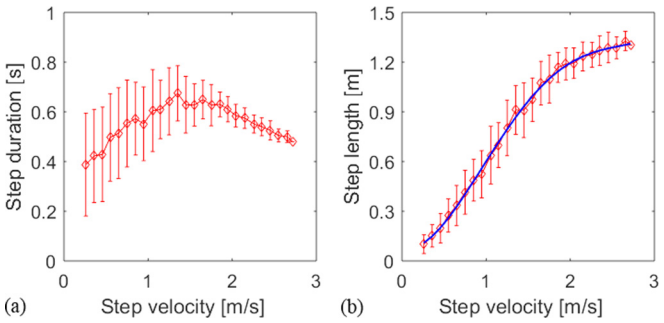

FIG. 8. (a) Binning result of step velocity-step duration samples. (b) Binning and fitting results of step velocity-step length samples.

suggests that the pedestrian's motion is weakly constrained by that of the predecessor and that pedestrians will react to the spatial constraint by adjusting their step length but not their step duration.

(c) Strongly constrained regime ($d < 0.71$ m). The step duration and step length both decrease sharply and linearly as the headway decreases. This finding suggests that the pedestrian's motion is strongly constrained by that of the predecessor and that pedestrians will react to the change in the spatial constraint by adjusting both their step length and step duration.

It is of particular interest that, at high densities [e.g., $N = 70$; see Fig. 3(g)], each round of motion for each pedestrian after a long stop often comprises a couple of continuous steps. Meanwhile, Fig. 5 shows that the duration and length of these steps are obviously shorter than those of the steps at low densities (e.g., $N = 10$). We refer to this phenomenon that arises spontaneously at high densities as the "self-organized small-step phenomenon." It forms because the space available ahead of the follower is very limited at high densities, so the follower cannot take a long step and must move with small steps. Another reason is the psychological effect whereby the follower will not take a long step that may risk a collision with the predecessor. This phenomenon also suggests that the follower will make efficient use of the available space and move in a timely fashion once a gap from the predecessor develops instead of waiting in place to take a preferred large step.

We compare our results on the relationships between headway and step duration and between headway and step length with the results of Zeng *et al.* [17] in Fig. 7. The relationship between headway and step length is basically similar, but the relationship between headway and step duration differs significantly and appears to be opposite that of the strongly constrained regime; their result shows that the step duration increases as the headway decreases. However, it is expected that if a large number of small steps with a short step duration can be detected at high densities (low headways), the average step duration will naturally decrease with the decrease in the headway. Thus, we speculate that the major reason is that the small steps that arise at high densities could not be tracked effectively with the head motion-based step measurement method used by Zeng *et al.* [17]. We elaborate on the reason in Sec. IV C.

B. Velocity-step duration relation and velocity-step length relation

Because the step velocity equals the step length divided by the step duration, the step velocity-step length and step velocity-step duration scatter data are easily obtained in terms of the samples data in Fig. 5. Figure 8 shows the results after the binning procedure is applied.

We were surprised to note that the step duration does not increase monotonously as the velocity decreases as reported in Refs. [12,14]; rather, it decreases as the velocity decreases within the relatively low velocity domain ($v < 1.35$ m/s). This is due to the increasing number of small steps that arise as the density increases (corresponding to the decrease in velocity) in the strongly constrained regime. The average step duration naturally decreases. The step duration is the longest at a velocity (v) of 1.35 m/s. The step duration decreases as the velocity increases within the relatively high velocity domain ($v \geqslant 1.35$ m/s) because pedestrians prefer to increase their velocity by shortening their step time to improve stepping efficiency in the free movement stage [14].

In addition, we note that the relationship between step velocity and step length seems to be more complex than that reported in Refs. [12,14]. We fit the results with a quartic function,

$$l = 0.08v^4 - 0.56v^3 + 1.17v^2 - 0.17v + 0.08, \quad (7)$$

where l and v represent the step length and step velocity, respectively.

Figure 9 compares the relationship between step length and step velocity with the results from previous studies [12,14,16,20,27]. Note that the focused motion object in this paper and in Refs. [20,27] is the foot, whereas, in Refs. [12,14,16], it is the head. Therefore, strictly speaking, their

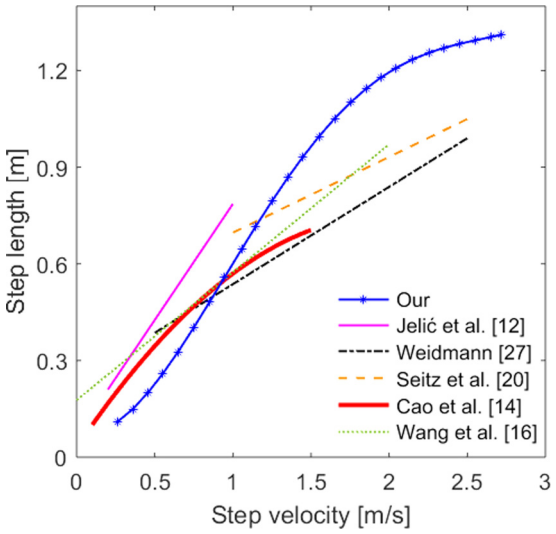

FIG. 9. Comparison of the relationship between step length and step velocity in our paper and in previous studies [12,14,16,20,27].

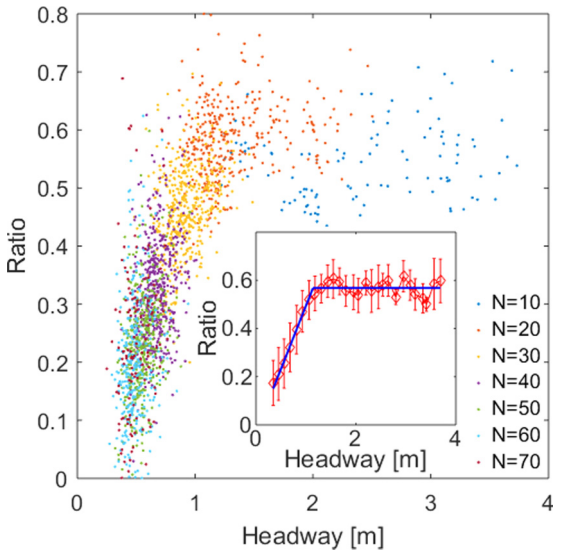

FIG. 10. Scatter diagram of 2476 headway-ratio samples. The inset shows the binning and fitting results.

results are not comparable. However, whether the head or the foot is used, the step length in our result is always smaller than those in Refs. [12,14,16] at the same velocity in the relatively low velocity domain. This is because the step duration in our paper is shorter than those in the previous studies at the same velocity in the relatively low velocity domain. The step length (i.e., velocity multiplied by duration) is naturally shorter than those in Refs. [12,14,16] at the same velocity. In the relatively high velocity domain, the step length in our paper is larger than those in Refs. [20,27]. Many factors, including the measurement method, experimental setup, and body characteristics, may contribute to this difference. In particular, the experimental subjects in Ref. [20] were not interacting pedestrians but isolated pedestrians, and the measurement appears to be manual rather than automatic, which may cause differences in the error level. In addition, they provided fewer step samples than we had in our paper. The critical reason for the difference with Ref. [27] is unclear because the details of the measurements were not given in Ref. [27].

C. Foot motion versus head motion

In this section, we address the relationship between head displacement and foot displacement during a step and whether the ratio between them equals 0.5 as often expected. Meanwhile, we address the question of why the small steps that arise at high densities are difficult to track effectively with the head motion-based step measurement method as in Refs. [12,14,16,17]. This question is key to interpreting the differences between this paper and previous studies [12,14,16,17] in the relationships between headway and step duration, between step velocity and step length, and between step velocity and step duration at high densities.

Because both head motion and foot motion were tracked in our experiment, we can compare the displacement of the head and foot during each step. In terms of the frame numbers of the start ($\tau^s_{i,k}$) and the end ($\tau^e_{i,k}$) of pedestrian i at the kth step, the longitudinal head displacement ($h_{i,k}$) of pedestrian i at the kth step can be easily calculated by

$$h_{i,k} = X_i(\tau^e_{i,k}) - X_i(\tau^s_{i,k}). \tag{8}$$

We then calculate the ratio (r) between the longitudinal head displacement and the foot displacement during each step. Figure 10 shows the headway-ratio scatter diagram. Surprisingly, the ratios are not fully equal to 0.5 as often expected. To obtain a clear headway-ratio relationship, we use a binning procedure to analyze the data and fit the result with the following piecewise function:

$$r = \begin{cases} 0.53d - 0.03, & \text{if } d < 1.14\,\text{m}, \\ 0.57, & \text{if } d \geqslant 1.14\,\text{m}, \end{cases} \tag{9}$$

When the headway $d < 1.14$ m, the ratio increases in a sharp and linear fashion as the headway increases. The ratio $r = 0.5$ when $d = 1$ m. When $d \geqslant 1.14$ m, the ratio remains constant ($r = 0.57$). This interesting result suggests that, when the distance to the predecessor is too short ($d < 1$ m), the pedestrian's body will deviate backward (i.e., the center of mass is closer to the rear foot than the front foot) to retain sufficient buffer space from the predecessor and thus avoid collision with the predecessor as illustrated in Fig. 11. When the distance to the predecessor is sufficiently long ($d \geqslant 1$ m), the pedestrian may no longer worry about a collision with the predecessor, and the pedestrian's body moves forward as much as possible and will deviate forward (i.e., the center of mass is closer to the front foot than the rear foot).

In terms of the headway-ratio relation and headway-step length relation [Fig. 6(a)], we know that both the ratio (r) and the foot displacement (l) during a small step may approach zero at high densities (low headways). The head displacement $L(= l \times r)$ during a small step will extremely approach zero. In other words, the head is nearly motionless. It is thus quite possible that the small steps that arise at high densities (low headways) could not be effectively detected with only a head motion-based step measurement method, such as those used in Refs. [12,14,16,17].

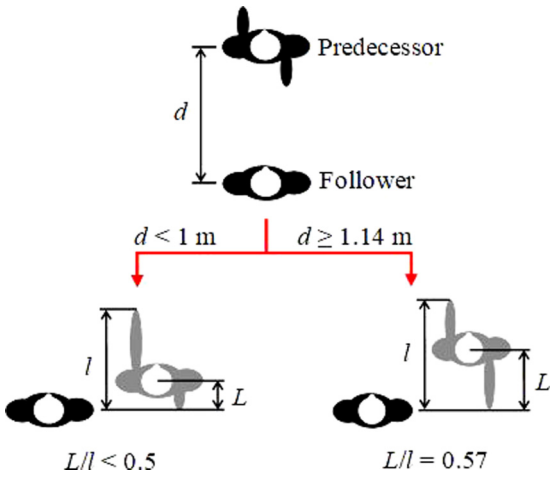

FIG. 11. Schematic of foot motion versus head motion during a step. The gray pedestrian represents the body posture of the follower after taking a step. When the headway is $d < 1$ m, the ratio is $L/l < 0.5$, and the pedestrian's body will deviate backward. When $d \geqslant 1.14$ m, the ratio remains constant at 0.57, and the pedestrian's body will deviate forward slightly.

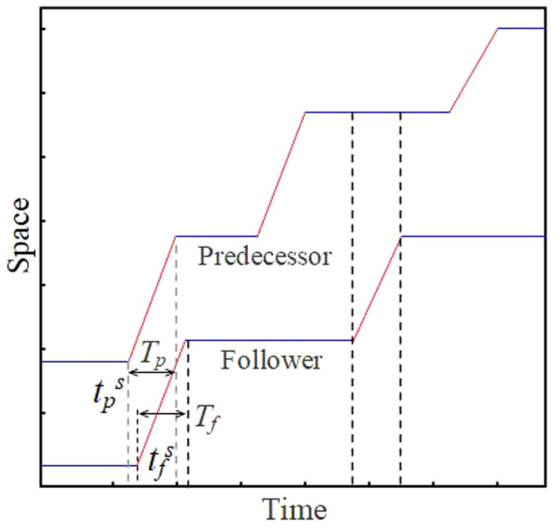

FIG. 12. Schematic of local synchronization and asynchronization phenomena in the exemplary time-space diagram of foot motion. Each fraction of oblique (red) line represents a step.

D. Step synchronization and asynchronization

In this section, we address the question of what density or headway results in the highest incidence of local step synchronization and asynchronization.

In terms of the time-space diagrams of foot motion (Fig. 3), it is easy to see that the marching-style step synchronization (i.e., global synchronization; all pedestrians step with the same step frequency and strictly in phase) is almost nonexistent. However, it is possible that two successive pedestrians step with the same step frequency and in phase (i.e., local step synchronization).

Jelić *et al.* [12] showed that local synchronization is observable at high densities and that local synchronization and antisynchronization (i.e., walking in phase with the opposite legs) exist simultaneously at low densities. This result was also confirmed by Wang *et al.* [16]. However, they did not indicate at which precise headway the incidence of local synchronization and asynchronization is highest, but they gave an approximate density range.

Because the start and end times of each step of each pedestrian were obtained by tracking foot motion, the phase difference between two successive pedestrians can be calculated easily and precisely. Specifically, the local synchronization of two successive pedestrians should satisfy two conditions: start time conformity and duration conformity.

(a) The start time conformity [i.e., the start times of the steps of the follower and the predecessor (t_f^s and t_p^s)] should satisfy $|t_f^s - t_p^s| \leqslant k$ as illustrated in the first step of the follower in Fig. 12. k is the relaxation variable about the time difference, which is set as 0.1 s in this paper.

(b) The duration conformity [i.e., the step durations of the steps of the follower and the predecessor (T_f and T_p)] should satisfy $|T_f - T_p| \leqslant k$. K is the relaxation variable about the duration difference, which is set as $(T_f + T_p)/8$ [12,16].

Only 255 pairs of successive pedestrians satisfy above two conditions and are considered to be synchronized in our experiment. The rejection ratio of the samples approaches 90%, which suggests that at least 90% of pairs of successive pedestrians are not synchronized. Figure 13(a) shows the probability density distribution (pdf) of headway in the detected synchronized 255 pairs of successive pedestrians. We fit the result with a three-parameter Burr distribution function,

$$f(d|\alpha, c, k) = \frac{(ck/\alpha)(d/\alpha)^{c-1}}{[1 + (d/\alpha)^c]^{k+1}}. \tag{10}$$

The parameters are estimated to be $\alpha = 0.75$, $c = 5.37$, and $k = 0.58$. In terms of the fitting result, the headway at the maxima of the pdf is calculated to be 0.76 m, which suggests that the local synchronization phenomenon is most likely to arise when the headway is 0.76 m. At this time, the local density is $1/0.76 = 1.31\,\mathrm{m}^{-1}$, which is basically consistent with the density range ($>1.25\,\mathrm{m}^{-1}$) given in Ref. [12].

We cannot detect an antisynchronization phenomenon (i.e., walking in phase with the opposite legs) in the experiment because the motion phase of the right leg is unknown. However, it is possible to investigate the local asynchronization phenomenon (i.e., the duration of the follower's step does not

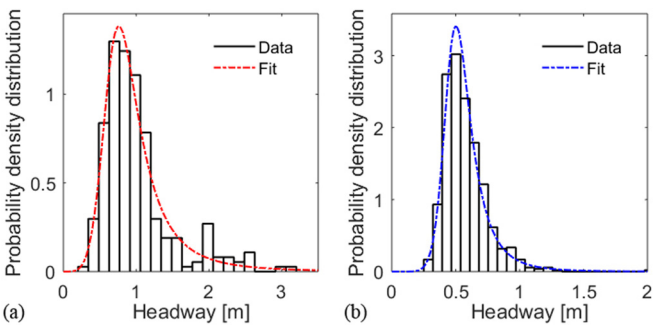

FIG. 13. Probability density distribution of headway for (a) the detected synchronized 255 pairs of successive pedestrians and (b) the asynchronous 745 pairs of successive pedestrians.

intersect with the duration of any of the predecessor's steps as illustrated in the second step of the follower in Fig. 12). In terms of this definition, 745 pairs of successive pedestrians are found to be asynchronous in our experiment. Figure 13(b) shows the pdf of the headway for the detected asynchronous 745 pairs of successive pedestrians. We also fit the result with a three-parameter Burr distribution function. The parameters were estimated to be $\alpha = 0.49$, $c = 8.51$, and $k = 0.58$. The headway at the maxima of the pdf is calculated as 0.51 m, which suggests that the asynchronization phenomenon is most likely to occur when the headway is 0.51 m. Note that this result seems to differ with that in Refs. [12,16]. One important reason is that the asynchronization defined in this paper is not equivalent to the antisynchronization discussed in Refs. [12,16].

V. CONCLUSIONS

In this paper, we present a pedestrian single-file movement experiment that directly captures the characteristics of the continuous stepping behaviors of pedestrians interacting in a crowd. Based on the experimental results, the following conclusions can be drawn.

First, the step length (duration) increases linearly as the headway increases and then remains constant when the headway exceeds 1.20 m (0.71 m). This result indicates that the relationship between step length (duration) and headway is piecewise linear and suggests the existence of three different regimes. The result also indicates that pedestrians' footsteps would change into small steps of short length and duration at high densities in the strongly constrained regime.

Second, the relationship between step duration and step velocity is nonmonotonous, and the step duration is the longest at a velocity of 1.35 m/s, whereas the relationship between step length and step velocity is monotonous and can be well represented by a quartic function.

Third, the dependency of the ratio between head displacement and foot displacement during a step on the headway is piecewise linear, and the ratio is less (greater) than 0.5 when the headway is shorter (longer) than 1 m. This result indicates that pedestrians' bodies usually deviate backward when the distance to the predecessor is too close (<1 m); conversely, they usually deviate forward when the distance is sufficiently long ($\geqslant 1$ m). In addition, this result can indirectly interpret the differences between this paper and the previous studies [12,14,16,17] in the relationships between headway and step duration, between step velocity and step length, and between step velocity and step duration at high densities.

Finally, step synchronization of two successive pedestrians is most likely to occur at a headway of 0.76 m. This conclusion is in line with the conclusions in Ref. [12]. Step asynchronization is most likely to occur at a headway of 0.51 m. A strict antisynchronization phenomenon [12] was not detected in our experiment because the motion of the pedestrians' right leg was not tracked. Further experiments are needed to answer this question in a future study.

Compared with previous studies of stepping dynamics [8–19], our experiment is the direct tracking of the interacting pedestrians' foot motion. This enables the stepping characteristics and phenomena to be investigated more efficiently and precisely. The main contribution of this paper is that it reveals many new stepping characteristics (e.g., the relationship between the headway and the ratio of head displacement and foot displacement in a step, the precise headways at which synchronization and asynchronization are most likely to arise) and phenomena (e.g., the forward- and backward-deviating phenomena of the body and the continuous small-step phenomena at high densities). These findings will greatly deepen our understanding of the basic stepping behavior of human beings.

ACKNOWLEDGMENTS

The authors acknowledge that this research was supported by the Fundamental Research Funds for the Central Universities, China.

[1] H. Kuang, X. Li, T. Song, and S. Dai, Analysis of pedestrian dynamics in counter flow via an extended lattice gas model, Phys. Rev. E **78**, 066117 (2008).

[2] D. Helbing, I. Farkas, and T. Vicsek, Simulating dynamical features of escape panic, Nature (London) **407**, 487 (2000).

[3] D. Helbing, L. Buzna, A. Johansson, and T. Werner, Self-organized pedestrian crowd dynamics: Experiments, simulations, and design solutions, Transport. Sci. **39**, 1 (2005).

[4] A. Seyfried, O. Passon, B. Steffen, M. Boltes, T. Rupprecht, and W. Klingsch, New insights into pedestrian flow through bottlenecks, Transport. Sci. **43**, 395 (2009).

[5] S. P. Hoogendoorn and W. Daamen, Pedestrian behavior at bottlenecks, Transport. Sci. **39**, 147 (2005).

[6] M. Moussaïd, E. G. Guillot, M. Moreau, J. Fehrenbach, O. Chabiron, S. Lemercier *et al.*, Traffic instabilities in self-organized pedestrian crowds, Plos Comput. Biol. **8**, e1002442 (2012).

[7] M. Moussaïd, D. Helbing, S. Garnier, A. Johansson, M. Combe, and G. Theraulaz, Experimental study of the behavioural mechanisms underlying self-organization in human crowds, Proc. R. Soc. B **276**, 2755 (2009).

[8] J. Zhang, W. Mehner, S. Holl, M. Boltes, E. Andresen, A. Schadschneider, and A. Seyfried, Universal flow-density relation of single-file bicycle, pedestrian and car motion, Phys. Lett. A **378**, 3274 (2014).

[9] A. Seyfried, B. Steffen, W. Klingsch, and M. Boltes, The fundamental diagram of pedestrian movement revisited, J. Stat. Mech.: Theory Exp. (2005) P10002.

[10] U. Chattaraj, A. Seyfried, and P. Chakroborty, Comparison of pedestrian fundamental diagram across cultures, Adv. Complex Syst. **12**, 393 (2009).

[11] A. Jelić, C. Appert-Rolland, S. Lemercier, and J. Pettré, Properties of pedestrians walking in line: fundamental diagrams, Phys. Rev. E **85**, 036111 (2012).

[12] A. Jelić, C. Appert-Rolland, S. Lemercier, and J. Pettré, Properties of pedestrians walking in line. II. Stepping behavior, Phys. Rev. E **86**, 046111 (2012).

[13] S. Cao, J. Zhang, D. Salden, J. Ma, C. Shi, and R. Zhang, Pedestrian dynamics in single-file movement of crowd with different age compositions, Phys. Rev. E **94**, 012312 (2016).

[14] S. Cao, J. Zhang, W. Song, C. Shi, and R. Zhang, The stepping behavior analysis of pedestrians from different age groups via a single-file experiment, J. Stat. Mech: Theory Exp. (2018) 033402.

[15] J. Wang, W. Weng, M. Boltes, J. Zhang, A. Tordeux, and V. Ziemer, Step styles of pedestrians at different densities, J. Stat. Mech.: Theory Exp. (2018) 023406.

[16] J. Wang, M. Boltes, A. Seyfried, J. Zhang, V. Ziemer, and W. Weng, Linking pedestrian flow characteristics with stepping locomotion, Physica A (Amsterdam) **500**, 106 (2018).

[17] G. Zeng, S. Cao, C. Liu, and W. Song, Experimental and modeling study on relation of pedestrian step length and frequency under different headways, Physica A (Amsterdam) **500**, 237 (2018).

[18] Z. M. Fang, W. G. Song, X. Liu, W. Lv, J. Ma, and X. Xiao, A continuous distance model (CDM) for the single-file pedestrian movement considering step frequency and length, Physica A (Amsterdam) **391**, 307 (2012).

[19] D. Yanagisawa, A. Tomoeda, and K. Nishinari, Improvement of pedestrian flow by slow rhythm, Phys. Rev. E **85**, 016111 (2012).

[20] M. J. Seitz and G. Köster, Natural discretization of pedestrian movement in continuous space, Phys. Rev. E **86**, 046108 (2012).

[21] M. J. Seitz, F. Dietrich, and G. Köster, The effect of stepping on pedestrian trajectories, Physica A (Amsterdam) **421**, 594 (2015).

[22] J. E. Bertram and A. Ruina, Multiple walking speed-frequency relations are predicted by constrained optimization, J. Theor. Biol. **209**, 445 (2001).

[23] L. V. Ojeda, J. R. Rebula, A. D. Kuo, and P. G. Adamczyk, Influence of contextual task constraints on preferred stride parameters and their variabilities during human walking, Med. Eng. Phys. **37**, 929 (2015).

[24] A. D. Kuo, A simple model of bipedal walking predicts the preferred speed-step length relationship, J. Biomech. Eng. **123**, 264 (2001).

[25] X. Liu, W. Song, and J. Zhang, Extraction and quantitative analysis of microscopic evacuation characteristics based on digital image processing, Physica A (Amsterdam) **388**, 2717 (2009).

[26] J. Ma, W. G. Song, Z. M. Fang, S. M. Lo, and G. X. Liao, Experimental study on microscopic moving characteristics of pedestrians in built corridor based on digital image processing, Build. Environ. **45**, 2160 (2010).

[27] U. Weidmann, *Transporttechnik der fussgänger* (Schriftenreihe des IVT 90, ETH Zürich, 1993), in German.